

1 **Covariance inflation in the ensemble Kalman filter: a residual**
2 **nudging perspective and some implications**

3 XIAODONG LUO *

International Research Institute Of Stavanger (IRIS), 5008 Bergen, Norway

4 IBRAHIM HOTEIT

King Abdullah University of Science and Technology (KAUST), Thuwal 23955-6900, Saudi Arabia

* *Corresponding author address:* International Research Institute Of Stavanger (IRIS), Thormøhlens Gate

55, 5008 Bergen, Norway

E-mail: xiaodong.luo@iris.no

ABSTRACT

This note examines the influence of covariance inflation on the distance between the measured observation and the simulated (or predicted) observation with respect to the state estimate. In order for the aforementioned distance to be bounded in a certain interval, some sufficient conditions are derived, indicating that the covariance inflation factor should be bounded in a certain interval, and that the inflation bounds are related to the maximum and minimum eigenvalues of certain matrices. Implications of these analytic results are discussed, and a numerical experiment is presented to verify the validity of our analysis.

1. Data assimilation with residual nudging

A finite, often small, ensemble size has some well known effects that may substantially influence the behaviour of an ensemble Kalman filter (EnKF). These effects include, for instance, rank deficient sample error covariance matrices, systematically underestimated error variances, and in contrast, exceedingly large error cross-covariances of the model state variables (Whitaker and Hamill 2002). In the literature, the latter two issues are often tackled through covariance localization (Hamill et al. 2001), while the first issue, under-estimation of sample variances, is often handled by covariance inflation (Anderson and Anderson 1999), in which one artificially increases the sample variances, either multiplicatively (see, for example, Anderson and Anderson 1999; Anderson 2007, 2009; Bocquet and Sakov 2012; Miyoshi 2011), or additively (see, for example, Hamill and Whitaker 2011), or in a hybrid way by combining both multiplicative and additive inflation methods (see, for example, Whitaker and Hamill 2012), or through other ways such as relaxation to the prior

26 (Zhang et al. 2004), multi-scheme ensembles (Meng and Zhang 2007), modification of the
 27 eigenvalues of sample error covariance matrices (Altaf et al. 2013; Luo and Hoteit 2011;
 28 Ott et al. 2004; Triantafyllou et al. 2013), back projection of the residuals to construct new
 29 ensemble members Song et al. (2010) to name but a few. In general, covariance inflation
 30 tends to increase the robustness of the EnKF against uncertainties in data assimilation
 31 (Luo and Hoteit 2011), and often also improves the filter performance in terms of estimation
 32 accuracy.

33 The focus of this note is to study the effect of covariance inflation from the point of
 34 view of residual nudging (Luo and Hoteit 2012). Here, the “residual” with respect to an
 35 m -dimensional system state \mathbf{x} is a vector in the observation space, defined as $\mathbf{H}\mathbf{x} - \mathbf{y}$ ¹,
 36 where $\mathbf{H} : \mathbb{R}^m \rightarrow \mathbb{R}^p$ is a linear observation operator, and \mathbf{y} the corresponding p -dimensional
 37 observation vector. Throughout this note, our discussion is confined to the filtering (or
 38 analysis) step of the EnKF, so that the time index in the EnKF is dropped. The linearity
 39 assumption in the observation operator \mathbf{H} is taken in order to simplify our discussion. The
 40 result to be presented later, though, might also provide insights into more complex situations.

41 Before introducing the concept of residual nudging, let us define some additional nota-
 42 tions. We assume that the observation system is given by

$$43 \quad \mathbf{y} = \mathbf{H}\mathbf{x} + \mathbf{v}, \tag{1}$$

44 where \mathbf{v} is the vector of observation error, with zero mean and a non-singular covariance
 45 matrix \mathbf{R} . We further decompose \mathbf{R} as $\mathbf{R} = \mathbf{R}^{1/2} \mathbf{R}^{T/2}$, where $\mathbf{R}^{1/2}$ is a non-singular square
 46 root of \mathbf{R} and $\mathbf{R}^{T/2}$ denotes the transpose of $\mathbf{R}^{1/2}$.

¹In the literature, the vector with the opposite sign, $\mathbf{y} - \mathbf{H}\mathbf{x}$, is often called “innovation”.

47 To measure the length of a vector \mathbf{z} in the observation space, we adopt the following
 48 weighted Euclidean norm

$$49 \quad \|\mathbf{z}\|_{\mathbf{R}} \equiv \sqrt{\mathbf{z}^T \mathbf{R}^{-1} \mathbf{z}}. \quad (2)$$

50 One may convert the weighted Euclidean norm to the standard Euclidean norm by noticing
 51 that $\|\mathbf{z}\|_{\mathbf{R}} = \|\mathbf{R}^{-1/2} \mathbf{z}\|_2$, where $\|\bullet\|_2$ denotes the standard Euclidean norm. As a result,
 52 many topological properties with respect to the standard Euclidean norm, e.g., the triangle
 53 inequality (see (3) below), still hold with respect to the weighted Euclidean norm.

54 The idea of data assimilation with residual nudging (DARN) is the following. Let \mathbf{x}^{tr}
 55 be the true system state (truth), $\mathbf{y}^o = \mathbf{H}\mathbf{x}^{tr} + \mathbf{v}^o$ the recorded observation for a specific
 56 realization \mathbf{v}^o of the observation error, and $\hat{\mathbf{x}}$ the state estimate (e.g., either the prior or
 57 posterior estimate) obtained from a data assimilation (DA) algorithm. Then the residual
 58 $\hat{\mathbf{r}} = \mathbf{H}\hat{\mathbf{x}} - \mathbf{y}^o = \mathbf{H}\hat{\mathbf{x}} - \mathbf{H}\mathbf{x}^{tr} - \mathbf{v}^o$. By the triangle inequality, the weighted Euclidean norm
 59 of the residual (residual norm hereafter) satisfies

$$60 \quad \|\hat{\mathbf{r}}\|_{\mathbf{R}} \leq \|\mathbf{H}\hat{\mathbf{x}} - \mathbf{H}\mathbf{x}^{tr}\|_{\mathbf{R}} + \|\mathbf{v}^o\|_{\mathbf{R}}. \quad (3)$$

61 If the DA algorithm performs reasonably well, one may expect that the magnitude of $\|\mathbf{H}\hat{\mathbf{x}} -$
 62 $\mathbf{H}\mathbf{x}^{tr}\|_{\mathbf{R}}$ not be significantly larger than $\|\mathbf{v}^o\|_{\mathbf{R}}$. As a result, one may obtain an upper bound
 63 of $\|\hat{\mathbf{r}}\|_{\mathbf{R}}$ in terms of $\|\mathbf{v}^o\|_{\mathbf{R}}$, e.g., in the form of $\beta\|\mathbf{v}^o\|_{\mathbf{R}}$, where β is a non-negative scalar
 64 coefficient. In practice, though, $\|\mathbf{v}^o\|_{\mathbf{R}}$ is often unknown. As a remedy, we replace $\|\mathbf{v}^o\|_{\mathbf{R}}$
 65 by an upper bound of the expectation $\mathbb{E}(\|\mathbf{v}\|_{\mathbf{R}})$ of the weighted Euclidean norm of the
 66 observation error \mathbf{v} , where \mathbb{E} denotes the expectation operator. One such upper bound can
 67 be obtained by noticing that

$$68 \quad (\mathbb{E}(\|\mathbf{v}\|_{\mathbf{R}}))^2 \leq \mathbb{E}(\|\mathbf{v}\|_{\mathbf{R}}^2) = \text{trace}(\mathbf{R}^{-1}\mathbb{E}(\mathbf{v}\mathbf{v}^T)) = \text{trace}(\mathbf{I}_p) = p, \quad (4)$$

69 where the operator “trace” evaluates the trace of a matrix, and \mathbf{I}_p the p -dimensional identity
70 matrix. From (4), we have the upper bound $\mathbb{E}(\|\mathbf{v}\|_{\mathbf{R}}) \leq \sqrt{p}$. Consequently, we want to find
71 a state estimate $\hat{\mathbf{x}}$ whose residual norm $\|\hat{\mathbf{r}}\|_{\mathbf{R}}$ satisfies

$$72 \quad \|\hat{\mathbf{r}}\|_{\mathbf{R}} \leq \beta\sqrt{p} \quad (5)$$

73 for a pre-chosen β . It is worthy of mentioning that in general it may be difficult to identify
74 which β gives the best state estimation accuracy with respect to the truth \mathbf{x}^{tr} . Therefore,
75 in Luo and Hoteit (2012) we mainly used DARN as a safeguard strategy, that is, if a state
76 estimate $\hat{\mathbf{x}}$ is found to have a too large residual norm, then we try to introduce some cor-
77 rection to the state estimate in order to reduce its residual norm, which in turn might also
78 improve the estimation accuracy.

79 In Luo and Hoteit (2012) we introduced DARN to the analysis $\hat{\mathbf{x}}^a$ in the ensemble ad-
80 justment Kalman filter (EAKF, see Anderson 2001). In the EAKF with residual nudging
81 (EAKF-RN), if the residual norm of $\hat{\mathbf{x}}^a$ is less than $\beta\sqrt{p}$, then we accept $\hat{\mathbf{x}}^a$ as a reasonable
82 estimate and no change is made. Otherwise, a correction is introduced to $\hat{\mathbf{x}}^a$ in a way such
83 that the residual norm of the modified state estimate $\tilde{\mathbf{x}}^a$ is exactly $\beta\sqrt{p}$, and that among
84 all possible state estimates whose residual norms are equal to $\beta\sqrt{p}$, the simulated (or pre-
85 dicted) observation $\mathbf{H}\tilde{\mathbf{x}}^a$ of the modified state estimate $\tilde{\mathbf{x}}^a$ has the shortest distance to the
86 one $\mathbf{H}\hat{\mathbf{x}}^a$ of the original state estimate $\hat{\mathbf{x}}^a$. Numerical results in Luo and Hoteit (2012) show
87 that the EAKF-RN exhibits (sometimes substantially) improved filter performance, in terms
88 of estimation accuracy and/or stability against filter divergence, compared to the EAKF.
89 Extension of DARN to other types of filters is also possible, for example, see Luo and Hoteit
90 (2013).

2. Covariance inflation from the point of view of residual nudging

Here we examine the effect of covariance inflation on the analysis residual norm. To this end, we first recall that the mean update formula in the EnKF (without perturbing the observation) is given by

$$\begin{aligned}\hat{\mathbf{x}}^a &= \hat{\mathbf{x}}^b + \mathbf{K} (\mathbf{y}^o - \mathbf{H}\hat{\mathbf{x}}^b) , \\ \mathbf{K} &= \hat{\mathbf{C}}^b \mathbf{H}^T (\mathbf{H}\hat{\mathbf{C}}^b \mathbf{H}^T + \mathbf{R})^{-1} ,\end{aligned}\tag{6}$$

where $\hat{\mathbf{x}}^b$ and $\hat{\mathbf{x}}^a$ are the sample means of the background and analysis ensembles, respectively; \mathbf{K} is the Kalman gain; and $\hat{\mathbf{C}}^b$ is a certain symmetric, positive semi-definite matrix in accordance to the chosen inflation scheme. In general $\hat{\mathbf{C}}^b$ may be related, but not necessarily proportional, to the sample error covariance matrix $\hat{\mathbf{P}}^b$ of the background ensemble. For instance, in the hybrid EnKF $\hat{\mathbf{C}}^b$ can be a mixture of $\hat{\mathbf{P}}^b$ and a “background covariance” \mathbf{B} (Hamill and Snyder 2000), or partially time-varying as in Hoteit et al. (2002).

Our objective is to examine under which conditions the residual norm $\|\hat{\mathbf{r}}^a\|_{\mathbf{R}}$ of the analysis $\hat{\mathbf{x}}^a$ satisfies $\beta_l \sqrt{p} \leq \|\hat{\mathbf{r}}^a\|_{\mathbf{R}} \leq \beta_u \sqrt{p}$, where β_l and β_u ($0 \leq \beta_l \leq \beta_u$) represents the lower and upper values of β that one wants to set for the analysis residual norm in DARN. Different from the previous works (Luo and Hoteit 2012, 2013), the lower bound $\beta_l \sqrt{p}$ is introduced here in order to make our discussion below slightly more general. In practice it may also be used to prevent too small residual norms in certain circumstances in order to avoid, for instance, a state estimate that over-fits the observation, a phenomenon that may be caused by “over-inflation”, as will be shown later.

111 Inserting Eq. (6) into $\hat{\mathbf{r}}^a = \mathbf{H}\hat{\mathbf{x}}^a - \mathbf{y}^o$, one has

$$112 \quad \hat{\mathbf{r}}^a = \mathbf{R} \left(\mathbf{H}\hat{\mathbf{C}}^b\mathbf{H}^T + \mathbf{R} \right)^{-1} \hat{\mathbf{r}}^b, \quad (7)$$

113 where $\hat{\mathbf{r}}^b = \mathbf{H}\hat{\mathbf{x}}^b - \mathbf{y}^o$. Multiplying both sides of Eq. (7) by $\mathbf{R}^{-1/2}$, one obtains

$$114 \quad (\mathbf{R}^{-1/2}\hat{\mathbf{r}}^a) = \left(\mathbf{R}^{-1/2}\mathbf{H}\hat{\mathbf{C}}^b\mathbf{H}^T\mathbf{R}^{-T/2} + \mathbf{I}_p \right)^{-1} (\mathbf{R}^{-1/2}\hat{\mathbf{r}}^b). \quad (8)$$

115 To derive the bounded residual norm, we first consider under which conditions the upper
116 bound $\|\hat{\mathbf{r}}^a\|_{\mathbf{R}} \leq \beta_u \sqrt{p}$ is guaranteed to hold. Given that (cf (19) later)

$$117 \quad \|\hat{\mathbf{r}}^a\|_{\mathbf{R}} = \|\mathbf{R}^{-1/2}\hat{\mathbf{r}}^a\|_2 \leq \|(\mathbf{R}^{-1/2}\mathbf{H}\hat{\mathbf{C}}^b\mathbf{H}^T\mathbf{R}^{-T/2} + \mathbf{I}_p)^{-1}\|_2 \|\hat{\mathbf{r}}^b\|_{\mathbf{R}}, \quad (9)$$

118 a sufficient condition is thus

$$119 \quad \|(\mathbf{R}^{-1/2}\mathbf{H}\hat{\mathbf{C}}^b\mathbf{H}^T\mathbf{R}^{-T/2} + \mathbf{I}_p)^{-1}\|_2 \leq \frac{\beta_u \sqrt{p}}{\|\hat{\mathbf{r}}^b\|_{\mathbf{R}}}. \quad (10)$$

120 Let

$$121 \quad \mathbf{A} = \mathbf{R}^{-1/2}\mathbf{H}\hat{\mathbf{C}}^b\mathbf{H}^T\mathbf{R}^{-T/2}, \quad (11)$$

122 and λ_{max} and λ_{min} be the maximum and minimum eigenvalues of \mathbf{A} , respectively. Recalling
123 that the induced 2-norm of a symmetric positive semi-definite matrix is exactly the maximum
124 eigenvalue of that matrix (Horn and Johnson 1990, §5.6.6), we have

$$125 \quad \|(\mathbf{A} + \mathbf{I}_p)^{-1}\|_2 = (\lambda_{min} + 1)^{-1}. \quad (12)$$

126 Therefore (10) leads to

$$127 \quad \lambda_{min} + 1 \geq \frac{\|\hat{\mathbf{r}}^b\|_{\mathbf{R}}}{\beta_u \sqrt{p}}. \quad (13)$$

128 If $\|\hat{\mathbf{r}}^b\|_{\mathbf{R}}$ is relatively small such that $\|\hat{\mathbf{r}}^b\|_{\mathbf{R}} \leq \beta_u \sqrt{p}$, then (13) automatically holds. How-
129 ever, if $\|\hat{\mathbf{r}}^b\|_{\mathbf{R}} > \beta_u \sqrt{p}$, and that λ_{min} is very small, then there is no guarantee that (13) will

130 hold. A small λ_{min} may appear, for instance, when the ensemble size n is smaller than the
 131 dimension p of the observation space. In such circumstances, the matrix \mathbf{A} may be singular
 132 with $\lambda_{min} = 0$, and the singularity may not be avoided only through the multiplicative co-
 133 variance inflation. If one cannot afford to increase the ensemble size n , then a few alternative
 134 strategies may be adopted to address (or at least mitigate) the problem of singularity. These
 135 include, for instance, (a) introducing covariance localization (Hamill et al. 2001) to $\hat{\mathbf{P}}^b$ in or-
 136 der to increase its rank (Hamill et al. 2009); (b) replacing the sample error covariance $\hat{\mathbf{P}}^b$ by
 137 a hybrid of $\hat{\mathbf{P}}^b$ and some full-rank matrix, similar to that in Hamill and Snyder (2000); and
 138 (c) reducing the dimension p of the observation in the update formula, for instance, by assim-
 139 ilating the observation in a serial way (see, for example, Whitaker and Hamill 2002), or by
 140 assimilating the observation in the framework of local EnKF (see, for example, Bocquet 2011;
 141 Ott et al. 2004). Once the problem of singularity is solved so that the smallest eigenvalue
 142 of \mathbf{A} becomes positive, a (large enough) multiplicative inflation factor can be introduced to
 143 make sure that (13) holds.

144 Inequality (13) provides insights of what the constraints there may be in choosing the
 145 inflation factor. In what follows, we study the problem in a slightly more general setting.
 146 Concretely, we consider a family of mean update formulae in the form of

$$147 \quad \hat{\mathbf{x}}^a = \hat{\mathbf{x}}^b + \mathbf{G} (\mathbf{y}^o - \mathbf{H}\hat{\mathbf{x}}^b) , \tag{14a}$$

$$148 \quad \mathbf{G} = \alpha \hat{\mathbf{C}}^b \mathbf{H}^T \left(\delta \mathbf{H} \hat{\mathbf{C}}^b \mathbf{H}^T + \gamma \mathbf{R} \right)^{-1} , \tag{14b}$$

150 where α , δ and γ are some positive coefficients, and \mathbf{G} is the gain matrix which in general
 151 differs from the Kalman gain \mathbf{K} in Eq. (6) with the presence of these three extra coeffi-
 152 cients. Without loss of generality, though, one may let $\alpha = 1$ (e.g., by moving α inside the

153 parentheses) so that the gain matrix is simplified to

$$154 \quad \mathbf{G} = \hat{\mathbf{C}}^b \mathbf{H}^T \left(\delta \mathbf{H} \hat{\mathbf{C}}^b \mathbf{H}^T + \gamma \mathbf{R} \right)^{-1}, \text{ with } \delta > 0 \text{ and } \gamma > 0. \quad (15)$$

155 If $\delta = 1$, then \mathbf{G} resembles the Kalman gain in the EnKF, with $1/\gamma$ being analogous to the
 156 multiplicative covariance inflation factor as used in Anderson and Anderson (1999). In our
 157 discussion below, we first derive some inflation constraints in the general case with $\delta > 0$,
 158 and then examine the more specific situation with $\delta = 1$. It is expected that one can also
 159 obtain constraints for other types of inflations in a similar way, but the results themselves
 160 may be case-dependent.

161 Using Eqs. (14a) and (15) as the update formulae and with some algebra, the weighted
 162 residual is given by

$$163 \quad (\mathbf{R}^{-1/2} \hat{\mathbf{r}}^a) = [\mathbf{I}_p - \mathbf{A} (\delta \mathbf{A} + \gamma \mathbf{I}_p)^{-1}] (\mathbf{R}^{-1/2} \hat{\mathbf{r}}^b), \quad (16)$$

164 where $\hat{\mathbf{r}}^a$, $\hat{\mathbf{r}}^b$ and \mathbf{A} are defined as previously. Let

$$165 \quad \begin{aligned} \Phi &\equiv \mathbf{I}_p - \mathbf{A} (\delta \mathbf{A} + \gamma \mathbf{I}_p)^{-1} \\ &= \frac{\delta - 1}{\delta} \mathbf{I}_p + \frac{\gamma}{\delta} (\delta \mathbf{A} + \gamma \mathbf{I}_p)^{-1}, \end{aligned} \quad (17)$$

166 then one has

$$167 \quad \|\hat{\mathbf{r}}^a\|_{\mathbf{R}} = \|\mathbf{R}^{-1/2} \hat{\mathbf{r}}^a\|_2 = \|\Phi (\mathbf{R}^{-1/2} \hat{\mathbf{r}}^b)\|_2. \quad (18)$$

168 For our purpose, the following two matrix inequalities are useful. Firstly, given a matrix \mathbf{M}
 169 and a vector \mathbf{z} with suitable dimensions, one has

$$170 \quad \|\mathbf{M} \mathbf{z}\|_2 \leq \|\mathbf{M}\|_2 \|\mathbf{z}\|_2, \quad (19)$$

171 where $\|\mathbf{M}\|_2$, the induced 2-norm of \mathbf{M} , is the maximum of the absolute singular values of
 172 \mathbf{M} , or equivalently, $\|\mathbf{M}\|_2$ is equal to the square root of the largest eigenvalue of $\mathbf{M} \mathbf{M}^T$

173 (Horn and Johnson 1990, ch. 5). Secondly, if in addition \mathbf{M} is non-singular, then (see, e.g.,
 174 Grcar 2010 and the references therein)

$$175 \quad \|\mathbf{M}^{-1}\|_2^{-1} \|\mathbf{z}\|_2 \leq \|\mathbf{M}\mathbf{z}\|_2. \quad (20)$$

176 The first inequality, (19), can be applied to obtain the sufficient conditions under which
 177 the inequality $\|\hat{\mathbf{r}}^a\|_{\mathbf{R}} \leq \beta_u \sqrt{p}$ is achieved. Let the maximum and minimum eigenvalues of Φ
 178 be μ_{max} and μ_{min} , respectively. Then by Eq. (17)

$$179 \quad \mu_{max} = \frac{\delta - 1}{\delta} + \frac{\gamma}{\delta} (\delta \lambda_{min} + \gamma)^{-1}, \quad (21a)$$

$$180 \quad \mu_{min} = \frac{\delta - 1}{\delta} + \frac{\gamma}{\delta} (\delta \lambda_{max} + \gamma)^{-1}. \quad (21b)$$

182 We remark that both μ_{max} and μ_{min} can be negative (e.g., when $\delta < 1$ and $\gamma \rightarrow 0$), therefore
 183 $\|\Phi\|_2 = \max(|\mu_{max}|, |\mu_{min}|)$. By (18) and (19), a sufficient condition for $\|\hat{\mathbf{r}}^a\|_{\mathbf{R}} \leq \beta_u \sqrt{p}$ is
 184 $\max(|\mu_{max}|, |\mu_{min}|) \leq \beta_u \sqrt{p} / \|\hat{\mathbf{r}}^b\|_{\mathbf{R}}$. For notational convenience, we define $\xi_u \equiv \beta_u \sqrt{p} / \|\hat{\mathbf{r}}^b\|_{\mathbf{R}}$
 185 and $\xi_l \equiv \beta_l \sqrt{p} / \|\hat{\mathbf{r}}^b\|_{\mathbf{R}}$.

186 Depending on the signs and magnitudes of μ_{max} and μ_{min} , there are in general four
 187 possible scenarios: (a) $\mu_{max} \geq 0$ and $\mu_{min} \geq 0$, so that $\|\Phi\|_2 = \mu_{max}$; (b) $\mu_{max} \leq 0$ and
 188 $\mu_{min} \leq 0$, so that $\|\Phi\|_2 = -\mu_{min}$; (c) $\mu_{max} \geq 0$, $\mu_{min} \leq 0$ and $\mu_{max} + \mu_{min} \geq 0$, so that
 189 $\|\Phi\|_2 = \mu_{max}$; and (d) $\mu_{max} \geq 0$, $\mu_{min} \leq 0$ and $\mu_{max} + \mu_{min} \leq 0$, so that $\|\Phi\|_2 = -\mu_{min}$.
 190 Inserting Eq. (21) into the above conditions one obtains some inequalities with respect to
 191 the variables δ and γ (subject to $\delta > 0$ and $\gamma > 0$), which are omitted in this note for brevity.

192 Similarly, the second inequality, (20), can be used to find the sufficient conditions for
 193 $\beta_l \sqrt{p} \leq \|\hat{\mathbf{r}}^a\|_{\mathbf{R}}$. By (18) and (20), one such sufficient condition can be $\|\Phi^{-1}\|_2 \leq \|\hat{\mathbf{r}}^b\|_{\mathbf{R}} / (\beta_l \sqrt{p}) =$
 194 $1/\xi_l$. By Eq. (17) it can be shown that

$$195 \quad \Phi^{-1} = \mathbf{I}_p + ((\delta - 1) \mathbf{I}_p + \gamma \mathbf{A}^{-1})^{-1}. \quad (22)$$

196 Let the maximum and minimum eigenvalues of Φ^{-1} be ν_{max} and ν_{min} , respectively, then

$$197 \quad \nu_{max} = 1 + \lambda_{max} ((\delta - 1) \lambda_{max} + \gamma)^{-1}, \quad (23a)$$

$$198 \quad \nu_{min} = 1 + \lambda_{min} ((\delta - 1) \lambda_{min} + \gamma)^{-1}. \quad (23b)$$

199
200 Similar to the previous discussion, we require that $\|\Phi^{-1}\|_2 = \max(|\nu_{max}|, |\nu_{min}|) \leq 1/\xi_l$,
201 which also leads to four possible scenarios: (a) $\nu_{max} \geq 0$ and $\nu_{min} \geq 0$, so that $\|\Phi^{-1}\|_2 =$
202 ν_{max} ; (b) $\nu_{max} \leq 0$ and $\nu_{min} \leq 0$, so that $\|\Phi^{-1}\|_2 = -\nu_{min}$; (c) $\nu_{max} \geq 0$, $\nu_{min} \leq 0$ and
203 $\nu_{max} + \nu_{min} \geq 0$, so that $\|\Phi^{-1}\|_2 = \nu_{max}$; and (d) $\nu_{max} \geq 0$, $\nu_{min} \leq 0$ and $\nu_{max} + \nu_{min} \leq 0$, so
204 that $\|\Phi^{-1}\|_2 = -\nu_{min}$. Again, inserting Eq. (23) into the above conditions one obtains some
205 inequalities with respect to the variables δ and γ .

206 Despite the complexity in the general situation, the analysis in the case of $\delta = 1$ (corre-
207 sponding to the update formula in the EnKF) is significantly simplified. Indeed, when $\delta = 1$,
208 the maximum and minimum eigenvalues in Eqs. (21) and (23) are all positive. Therefore
209 the following conditions

$$210 \quad \mu_{max} = \gamma (\lambda_{min} + \gamma)^{-1} \leq \xi_u, \quad (24a)$$

$$211 \quad \nu_{max} = 1 + \lambda_{max}/\gamma \leq 1/\xi_l. \quad (24b)$$

212
213 are sufficient for the objective $\beta_l \sqrt{p} \leq \|\hat{\mathbf{r}}^a\|_{\mathbf{R}} \leq \beta_u \sqrt{p}$. Note that if $\xi_u \geq 1$, i.e., $\|\hat{\mathbf{r}}^b\|_{\mathbf{R}} \leq$
214 $\beta_u \sqrt{p}$, then any $\gamma > 0$ would guarantee that $\|\hat{\mathbf{r}}^a\|_{\mathbf{R}} \leq \beta_u \sqrt{p}$ (indeed by Eqs. (16) and (19))
215 the analysis residual norm $\|\hat{\mathbf{r}}^a\|_{\mathbf{R}}$ is guaranteed to be no larger than $\|\hat{\mathbf{r}}^b\|_{\mathbf{R}}$ since $\|\Phi\|_2 \leq 1$
216 with $\delta = 1$), and that inequality (24a) holds. On the other hand, if $\xi_l \geq 1$ such that
217 $\|\hat{\mathbf{r}}^b\|_{\mathbf{R}} \leq \beta_l \sqrt{p}$, then in most cases² it is impossible for the EnKF to have $\|\hat{\mathbf{r}}^a\|_{\mathbf{R}}$ no less

²An exception is in the case that $\gamma = +\infty$ and $\xi_l = 1$. This implies that $\|\hat{\mathbf{r}}^a\|_{\mathbf{R}} = \|\hat{\mathbf{r}}^b\|_{\mathbf{R}} = \beta_l \sqrt{p}$, and that no mean update is conducted (i.e., $\hat{\mathbf{x}}^a = \hat{\mathbf{x}}^b$).

218 than $\|\hat{\mathbf{r}}^b\|_{\mathbf{R}}$ (hence $\beta_l \sqrt{p}$), for the same aforementioned reason. Therefore the inequality
 219 (24b) becomes infeasible. With these said, in what follows we focus on the cases in which
 220 $\xi_u, \xi_l \in [0, 1)$. With some algebra, it can be shown that γ should be bounded by

$$221 \quad \frac{\xi_l}{1 - \xi_l} \lambda_{max} \leq \gamma \leq \frac{\xi_u}{1 - \xi_u} \lambda_{min}. \quad (25)$$

222 Let $\kappa = \lambda_{max}/\lambda_{min}$ be the condition number of the (normalized) matrix $\mathbf{A} = \mathbf{R}^{-1/2} \mathbf{H} \hat{\mathbf{C}}^b \mathbf{H}^T \mathbf{R}^{-T/2}$.

223 From (25) we have $\frac{\xi_l}{1 - \xi_l} \lambda_{max} \leq \frac{\xi_u}{1 - \xi_u} \lambda_{min}$, which leads to a constraint in choosing β_l and
 224 β_u , in terms of

$$225 \quad \beta_l \leq \frac{\beta_u}{\kappa + (1 - \kappa) \xi_u}. \quad (26)$$

226 Inequality (25) suggests that the upper and lower bounds of γ are related to the min-
 227 imum and maximum eigenvalues of \mathbf{A} , respectively. In particular, to avoid a too small
 228 residual norm, i.e., observation over-fitting, γ should be lower bounded, hence its inverse
 229 $1/\gamma$, resembling the multiplicative inflation factor, should be upper bounded, as mentioned
 230 previously.

231 In practice, if the dimension p of the observation space is large, then it may be expensive
 232 to evaluate λ_{max} and λ_{min} . In certain circumstances, though, there may be cheaper ways to
 233 compute an interval for γ . For instance, if $\hat{\mathbf{C}}^b$ in the mean update formula is in the form
 234 of $c_1 \hat{\mathbf{P}}^b + c_2 \mathbf{B}$ with c_1 and c_2 being some positive scalars and \mathbf{B} a constant, symmetric and
 235 positive-definite matrix, then

$$236 \quad \mathbf{A} = c_1 \mathbf{R}^{-1/2} \mathbf{H} \hat{\mathbf{P}}^b \mathbf{H}^T \mathbf{R}^{-T/2} + c_2 \mathbf{R}^{-1/2} \mathbf{H} \mathbf{B} \mathbf{H}^T \mathbf{R}^{-T/2}.$$

237 The additive Weyl inequality (Horn and Johnson 1991, ch. 3) suggests that the following

238 bounds hold for λ_{max} and λ_{min} .

$$\lambda_{max} \leq c_1 \tau_{max} + c_2 \rho_{max}, \quad (27)$$

$$\lambda_{min} \geq c_1 \tau_{min} + c_2 \rho_{min} \geq c_2 \rho_{min},$$

239
 240 where τ and ρ are the eigenvalues of $\mathbf{R}^{-1/2} \mathbf{H} \hat{\mathbf{P}}^b \mathbf{H}^T \mathbf{R}^{-T/2}$ and $\mathbf{R}^{-1/2} \mathbf{H} \mathbf{B} \mathbf{H}^T \mathbf{R}^{-T/2}$, respec-
 241 tively. In many situations, $\hat{\mathbf{P}}^b$ may be rank deficient, therefore a singular value decomposition
 242 (SVD) analysis shows that τ_{max} is equal to the largest eigenvalue of $(\mathbf{H} \hat{\mathbf{S}}^b)^T \mathbf{R}^{-1} (\mathbf{H} \hat{\mathbf{S}}^b)$, where
 243 $\hat{\mathbf{S}}^b$ is a square root of $\hat{\mathbf{P}}^b$ that can be directly constructed based on the background ensemble
 244 (Bishop et al. 2001; Luo and Moroz 2009; Wang et al. 2004). Note that $(\mathbf{H} \hat{\mathbf{S}}^b)^T \mathbf{R}^{-1} (\mathbf{H} \hat{\mathbf{S}}^b)$ is
 245 a matrix with its dimension determined by the ensemble size n , and is in fact the same as the
 246 one used in the ensemble transform Kalman filter (ETKF) (Bishop et al. 2001; Wang et al.
 247 2004) in order to obtain the transform matrix. Therefore τ_{max} can be taken as a by-product
 248 in the framework of ETKF. On the other hand, if both \mathbf{H} and \mathbf{R} are time-invariant, then
 249 the eigenvalues ρ_{max} and ρ_{min} of $\mathbf{R}^{-1/2} \mathbf{H} \mathbf{B} \mathbf{H}^T \mathbf{R}^{-T/2}$ can be calculated off-line once and for
 250 all. Taking these considerations into account, (25) can be modified as follows

$$\frac{\xi_l}{1 - \xi_l} (c_1 \tau_{max} + c_2 \rho_{max}) \leq \gamma \leq \frac{\xi_u}{1 - \xi_u} (c_2 \rho_{min}). \quad (28)$$

252 Accordingly, (26) is changed to

$$\beta_l \leq \frac{\beta_u}{\tilde{\kappa} + (1 - \tilde{\kappa}) \xi_u}, \quad (29)$$

254 with $\tilde{\kappa} = (c_1 \tau_{max} + c_2 \rho_{max}) / (c_2 \rho_{min})$ being a modified ‘‘condition number’’.

255 **Remark:** Inequalities (25) and (26), or alternatively, (28) and (29), are sufficient, but not
 256 necessary, conditions. Therefore, even though γ does not lie in the interval in (25) or (28),

257 it may be still possible for the analysis residual norm to satisfy $\beta_l \sqrt{p} \leq \|\hat{\mathbf{r}}^a\|_{\mathbf{R}} \leq \beta_u \sqrt{p}$.

3. Numerical verification

Here we focus on using the 40-dimensional Lorenz 96 (L96) model (Lorenz and Emanuel 1998) to verify the above analytic results, while more intensive filter (with residual nudging) performance investigations are reported in Luo and Hoteit (2012). The experiment settings are the following. A reference trajectory (truth) is generated by numerically integrating the L96 model (with the driving force term $F = 8$) forward through the fourth-order Runge-Kutta method, with the integration step being 0.05 and the total number of integration steps being 1500. The first 500 steps are discarded to avoid the transition effect, and the rest 1000 steps are used for data assimilation. To obtain a long-term “background covariance” \mathbf{B}^{lt} (“background mean” \mathbf{x}^B , respectively), we also conduct a separate long model run with 100,000 integration steps, and take \mathbf{B}^{lt} (\mathbf{x}^B) as the temporal covariance (mean) of the generated model trajectory. The synthetic observations are generated by adding the Gaussian white noise $N(0, 1)$ to each odd number elements (x_1, x_3, \dots, x_{39}) of the state vector $\mathbf{x} = [x_1, x_2, \dots, x_{40}]^T$ every 4 integration steps. This corresponds to the 1/2 observation scenario used in Luo and Hoteit (2012). An initial ensemble with 20 ensemble members is generated by drawing samples from the Gaussian distribution $N(\mathbf{x}^B, \mathbf{B}^{lt})$, and the ETKF is adopted for data assimilation.

For distinction later, we call the ETKF without residual nudging the normal ETKF, and the ETKF with residual nudging the ETKF-RN. In the normal ETKF, Eq. (6) is used for mean update with $\hat{\mathbf{C}}^b$ equal to the sample error covariance $\hat{\mathbf{P}}^b$ of the background ensemble³. Neither covariance inflation nor covariance localization is introduced to the normal

³One may also let $\hat{\mathbf{C}}^b$ be the hybrid of $\hat{\mathbf{P}}^b$ and \mathbf{B}^{lt} . In this case, both residual norms and root mean square errors (RMSEs) of the normal ETKF may become smaller (results not shown), while the validity of

ETKF, since for our purpose we wish to use this plain filter setting as the baseline for comparison. One may adopt various inflation and localization techniques to enhance the filter performance, but such an investigation is beyond the scope of this note.

In the ETKF-RN, we adopt the hybrid scheme $\hat{\mathbf{C}}^b = 0.5\hat{\mathbf{P}}^b + 0.5\mathbf{B}^{lt}$ to address the issue of possible singularity in the matrix \mathbf{A} (cf. Eq. 11). Eq. (14) is adopted for mean update, with $\alpha = \delta = 1$, and γ constrained by (28) and (29). For convenience, we denote the lower and upper bounds of γ in (28) by γ_{min} and γ_{max} , respectively, and re-write γ in terms of $\gamma = \gamma_{min} + c(\gamma_{max} - \gamma_{min})$ with c being a corresponding scalar coefficient that is involved in our discussion later. Note that in general the background residual norm $\|\hat{\mathbf{r}}^b\|_{\mathbf{R}}$ changes with time, so are the values of ξ_u and ξ_l in Eq. (25). This implies that in general γ_{min} and γ_{max} (hence γ) also change with time, therefore they need to be calculated at each data assimilation cycle.

An additional remark is that the normal ETKF and the ETKF-RN share the same square root update formula as in Wang et al. (2004), where it is the sample error covariance $\hat{\mathbf{P}}^b$, rather than its hybrid with \mathbf{B}^{lt} , which is used to generate the background square root. Such a choice is based on the following considerations. On the one hand, if one uses the hybrid covariance for square root update, then it would require a matrix factorization (e.g., singular value decomposition) in order to compute a square root of the hybrid covariance at each data assimilation cycle, which can be very expensive in large-scale applications. On the other hand, for the L96 model used here, numerical investigations show that using the hybrid covariance for square root update does not necessarily improve the filter performance (results not shown).

the analytic results in the previous section is not affected.

301 The procedures in the ETKF-RN are summarized as follows. Because the matrix $\mathbf{R}^{-1/2}\mathbf{H}\mathbf{B}\mathbf{H}^T\mathbf{R}^{-T/2}$
 302 is time invariant, its maximum and minimum eigenvalues, ρ_{max} and ρ_{min} (cf. (28)), respec-
 303 tively, are calculated and saved for later use. Then, with the background ensemble at each
 304 data assimilation cycle, calculate the sample mean $\hat{\mathbf{x}}^b$, the corresponding background residual
 305 norm $\|\hat{\mathbf{r}}^b\|_{\mathbf{R}}$, and a square root $\hat{\mathbf{S}}^b$ of the sample error covariance $\hat{\mathbf{P}}^b$ following Bishop et al.
 306 (2001); Luo and Moroz (2009); Wang et al. (2004). Update $\hat{\mathbf{S}}^b$ to its analysis counterpart
 307 $\hat{\mathbf{S}}^a \equiv \hat{\mathbf{S}}^b\mathbf{T}\mathbf{U}$ by calculating a transform matrix \mathbf{T} , together with a “centering” matrix \mathbf{U}
 308 following Wang et al. (2004). During the square root update process, the maximum eigen-
 309 value τ_{max} of $\mathbf{R}^{-1/2}\mathbf{H}\hat{\mathbf{P}}^b\mathbf{H}^T\mathbf{R}^{-T/2}$ is obtained as a by-product following our discussion in the
 310 previous section. With these information, one is ready to calculate the interval bounds γ_{min}
 311 and γ_{max} in (28), hence obtain $\gamma = \gamma_{min} + c(\gamma_{max} - \gamma_{min})$ for a given value of c (c can be
 312 constant or variable during the whole data assimilation time window). This γ value is then
 313 inserted into Eq. (14) (with $\alpha = \delta = 1$ there) to obtain the analysis mean $\hat{\mathbf{x}}^a$. With $\hat{\mathbf{x}}^a$
 314 and $\hat{\mathbf{S}}^a$, an analysis ensemble can be generated in the same way as in Bishop et al. (2001);
 315 Wang et al. (2004). Propagating this ensemble forward in time, one starts a new data as-
 316 simulation cycle, and so on. Comparing the above procedures to those in Luo and Hoteit
 317 (2012), the observation inversion used in Luo and Hoteit (2012) is avoided.

318 The experiment below aims to show that, at each data assimilation cycle, if a γ value
 319 lies in the interval $\mathbb{C}_\gamma = [\gamma_{min}, \gamma_{max}]$ given by (28), then the corresponding analysis residual
 320 norm $\|\hat{\mathbf{r}}^a\|_{\mathbf{R}}$ is bounded by the interval $\mathbb{C}_{rn} = [\beta_l\sqrt{p}, \beta_u\sqrt{p}]$, with β_l and β_u satisfying the
 321 constraint (29). In the experiment we fix $\beta_u = 2$, and let $\beta_l = 0.1 \times (\beta_u/(\tilde{\kappa} + (1 - \tilde{\kappa})\xi_u))$,
 322 where the small fraction 0.1 is introduced for convenience of visualization⁴.

⁴In some cases $\beta_u/(\tilde{\kappa} + (1 - \tilde{\kappa})\xi_u)$ in (29) may be very close to β_u . Therefore if β_l is close to this value,

323 Fig. 1 shows the time series of the background (dash-dotted) and analysis (thick solid)
 324 residual norms in different filter settings (for convenience of visualization, the residual norm
 325 values are plotted in the logarithmic scale). For reference we also plot the targeted lower and
 326 upper bounds (dash and thin solid lines, respectively), $\beta_l\sqrt{p}$ and $\beta_u\sqrt{p}$ ($p = 20$), respectively.
 327 In the normal ETKF (Fig. 1(a)), in most of the time the analysis residual norms are larger
 328 than the targeted upper bound (no targeted lower bound is calculated and plotted in this
 329 case). With residual nudging, the analysis residual norms of the ETKF-RN migrate into
 330 the targeted interval, as long as the coefficient c lies in $[0, 1]$ (Figs. 1(b) – 1(d). Also see
 331 the caption of Fig. 1 to find out how the corresponding c values are chosen). When c is
 332 outside the interval $[0, 1]$, the corresponding γ is not bounded by $[\gamma_{min}, \gamma_{max}]$, hence there is
 333 no guarantee that the corresponding analysis residual norms are bounded by $[\beta_l\sqrt{p}, \beta_u\sqrt{p}]$.
 334 Two such examples are presented in Fig. 1(e) and 1(f), with c being 2.5 and -0.005 ,
 335 respectively (e.g., for $c = -0.005$ in Fig. 1(f), breakthroughs of the lower bound are found
 336 around time step 220 and a few other places). As side results, we also report in Table 1 the
 337 time mean root mean square errors (RMSEs) (see Eq. (13) of Luo and Hoteit 2012) that
 338 correspond to different filter settings in Fig. 1. In these tested cases, the filter performance
 339 of the ETKF-RN appears improved, in terms of the time mean RMSE, when compared to
 340 that of the normal ETKF.

the difference $(\beta_u - \beta_l)$, hence the interval \mathbb{C}_{rn} , may be very small.

341 4. Discussion and conclusion

342 We derived some sufficient inflation constraints in order for the analysis residual norm
343 to be bounded in a certain interval. The analytic results showed that these constraints
344 are related to the maximum and minimum eigenvalues of certain matrices (cf. Eq. (11)).
345 In certain circumstances, the constraint with respect to the minimum eigenvalue (e.g., Eq.
346 (13)) may impose a non-singularity requirement on relevant matrices. A few strategies in
347 the literature that can be adopted to address or mitigate this issue are highlighted.

348 Some remaining issues are manifest in our deduction. These include, for instance, the
349 nonlinearity in the observation operator and the choice of β_u and β_l . For the former prob-
350 lem, under a suitable smoothness assumption on the observation operator, one may also
351 obtain inflation constraints similar to those in Section 2. On the other hand, though, more
352 investigations may be needed to make the results more practical in terms of computational
353 complexity. For the latter problem, numerical results in Luo and Hoteit (2012) show that
354 the β values influence the overall performance of the EnKF in terms of filter stability and
355 accuracy. Intuitively, smaller (larger) β values tend to make residual nudging happen more
356 (less) often. Therefore, if the normal EnKF performs well (poorly), then a larger (smaller)
357 β value may be suitable. In this aspect, it is expected that an objective criterion is needed.
358 This will be investigated in the future.

Acknowledgement

We would like to thank two anonymous reviewers for their constructive comments and suggestions. The first author would also like to thank the IRIS/CIPR cooperative research project “Integrated Workflow and Realistic Geology” which is funded by industry partners ConocoPhillips, Eni, Petrobras, Statoil, and Total, as well as the Research Council of Norway (PETROMAKS) for financial support.

REFERENCES

- Altaf, U. M., T. Butler, X. Luo, C. Dawson, T. Mayo, and H. Hoteit, 2013: Improving short range ensemble Kalman storm surge forecasting using robust adaptive inflation. *Mon. Wea. Rev.*, accepted.
- Anderson, J. L., 2001: An ensemble adjustment Kalman filter for data assimilation. *Mon. Wea. Rev.*, **129**, 2884–2903.
- Anderson, J. L., 2007: An adaptive covariance inflation error correction algorithm for ensemble filters. *Tellus*, **59A (2)**, 210–224.
- Anderson, J. L., 2009: Spatially and temporally varying adaptive covariance inflation for ensemble filters. *Tellus*, **61A**, 72–83.
- Anderson, J. L. and S. L. Anderson, 1999: A Monte Carlo implementation of the nonlinear

377 filtering problem to produce ensemble assimilations and forecasts. *Mon. Wea. Rev.*, **127**,
378 2741–2758.

379 Bishop, C. H., B. J. Etherton, and S. J. Majumdar, 2001: Adaptive sampling with ensemble
380 transform Kalman filter. Part I: theoretical aspects. *Mon. Wea. Rev.*, **129**, 420–436.

381 Bocquet, M., 2011: Ensemble Kalman filtering without the intrinsic need for inflation. *Non-*
382 *linear Processes in Geophysics*, **18 (5)**, 735–750.

383 Bocquet, M. and P. Sakov, 2012: Combining inflation-free and iterative ensemble Kalman
384 filters for strongly nonlinear systems. *Nonlinear Processes in Geophysics*, **19 (3)**, 383–399.

385 Grear, J. F., 2010: A matrix lower bound. *Linear Algebra and its Applications*, **433**, 203–220.

386 Hamill, T. M. and C. Snyder, 2000: A hybrid ensemble Kalman filter-3d variational analysis
387 scheme. *Mon. Wea. Rev.*, **128**, 2905–2919.

388 Hamill, T. M. and J. S. Whitaker, 2011: What constrains spread growth in forecasts initial-
389 ized from ensemble Kalman filters? *Mon. Wea. Rev.*, **139**, 117–131.

390 Hamill, T. M., J. S. Whitaker, J. L. Anderson, and C. Snyder, 2009: Comments on “Sigma-
391 point Kalman filter data assimilation methods for strongly nonlinear systems”. *J. Atmos.*
392 *Sci.*, **66**, 3498–3500.

393 Hamill, T. M., J. S. Whitaker, and C. Snyder, 2001: Distance-dependent filtering of back-
394 ground error covariance estimates in an ensemble Kalman filter. *Mon. Wea. Rev.*, **129**,
395 2776–2790.

396 Horn, R. and C. Johnson, 1990: *Matrix analysis*. Cambridge University Press.

- 397 Horn, R. and C. Johnson, 1991: *Topics in matrix analysis*. Cambridge University Press.
- 398 Hoteit, I., D. T. Pham, and J. Blum, 2002: A simplified reduced order Kalman filtering and
399 application to altimetric data assimilation in Tropical Pacific. *Journal of Marine Systems*,
400 **36**, 101–127.
- 401 Lorenz, E. N. and K. A. Emanuel, 1998: Optimal sites for supplementary weather observa-
402 tions: Simulation with a small model. *J. Atmos. Sci.*, **55**, 399–414.
- 403 Luo, X. and I. Hoteit, 2011: Robust ensemble filtering and its relation to covariance inflation
404 in the ensemble Kalman filter. *Mon. Wea. Rev.*, **139**, 3938–3953.
- 405 Luo, X. and I. Hoteit, 2012: Ensemble Kalman filtering with residual nudging. *Tellus A*, **64**,
406 17 130.
- 407 Luo, X. and I. Hoteit, 2013: Efficient particle filtering through residual nudging. *Quart. J.*
408 *Roy. Meteor. Soc.*, in press.
- 409 Luo, X. and I. M. Moroz, 2009: Ensemble Kalman filter with the unscented transform.
410 *Physica D*, **238**, 549–562.
- 411 Meng, Z. and F. Zhang, 2007: Tests of an ensemble Kalman filter for mesoscale and regional-
412 scale data assimilation. part II: Imperfect model experiments. *Mon. Wea. Rev.*, **135** (4),
413 1403–1423.
- 414 Miyoshi, T., 2011: The Gaussian approach to adaptive covariance inflation and its imple-
415 mentation with the local ensemble transform Kalman filter. *Monthly Weather Review*,
416 **139**, 1519–1535.

- 417 Ott, E., et al., 2004: A local ensemble Kalman filter for atmospheric data assimilation.
418 *Tellus*, **56A**, 415–428.
- 419 Song, H., I. Hoteit, B. Cornuelle, and A. Subramanian, 2010: An adaptive approach to
420 mitigate background covariance limitations in the ensemble Kalman filter. *Mon. Wea.*
421 *Rev.*, **138 (7)**, 2825–2845.
- 422 Triantafyllou, G., I. Hoteit, X. Luo, K. Tsiaras, and G. Petihakis, 2013: Assessing a robust
423 ensemble-based Kalman filter for efficient ecosystem data assimilation of the Cretan sea.
424 *Journal of Marine Systems*, in press.
- 425 Wang, X., C. H. Bishop, and S. J. Julier, 2004: Which is better, an ensemble of positive-
426 negative pairs or a centered simplex ensemble. *Mon. Wea. Rev.*, **132**, 1590–1605.
- 427 Whitaker, J. S. and T. M. Hamill, 2002: Ensemble data assimilation without perturbed
428 observations. *Mon. Wea. Rev.*, **130**, 1913–1924.
- 429 Whitaker, J. S. and T. M. Hamill, 2012: Evaluating methods to account for system errors
430 in ensemble data assimilation. *Monthly Weather Review*, **140**, 3078–3089.
- 431 Zhang, F., C. Snyder, and J. Sun, 2004: Impacts of initial estimate and observation avail-
432 ability on convective-scale data assimilation with an ensemble Kalman filter. *Mon. Wea.*
433 *Rev.*, **132 (5)**, 1238–1253.

434 **List of Tables**

435 1 Time mean RMSEs in the normal ETKF and the ETKF-RN with the same c
436 values as in Fig. 1. 23

TABLE 1. Time mean RMSEs in the normal ETKF and the ETKF-RN with the same c values as in Fig. 1.

	Normal ETKF	ETKF-RN with				
		$c = 0$	$c = 1$	$c \in [0, 1]$	$c = 2.5$	$c = -0.005$
Background RMSE	4.3148	1.8252	2.4095	2.2182	2.6857	2.0394
Analysis RMSE	4.2645	1.6953	2.2764	2.0894	2.5679	1.9054

437 List of Figures

438 1 Time series of the analysis residual norms in: (a): the normal ETKF without
439 residual nudging; (b) – (f) the ETKF-RN with different c values. For the
440 normal ETKF there are no targeted lower and upper residual norm bounds.
441 For reference, though, we still plot the targeted upper bound ($= 2\sqrt{20}$) in (a).
442 We also note that the c value in Fig. 1(d) is randomly drawn from the uniform
443 distribution on the interval $[0, 1]$ at each data assimilation cycle, while in the
444 rest of the sub-figures the c values are constant during the assimilation time
445 window.

25

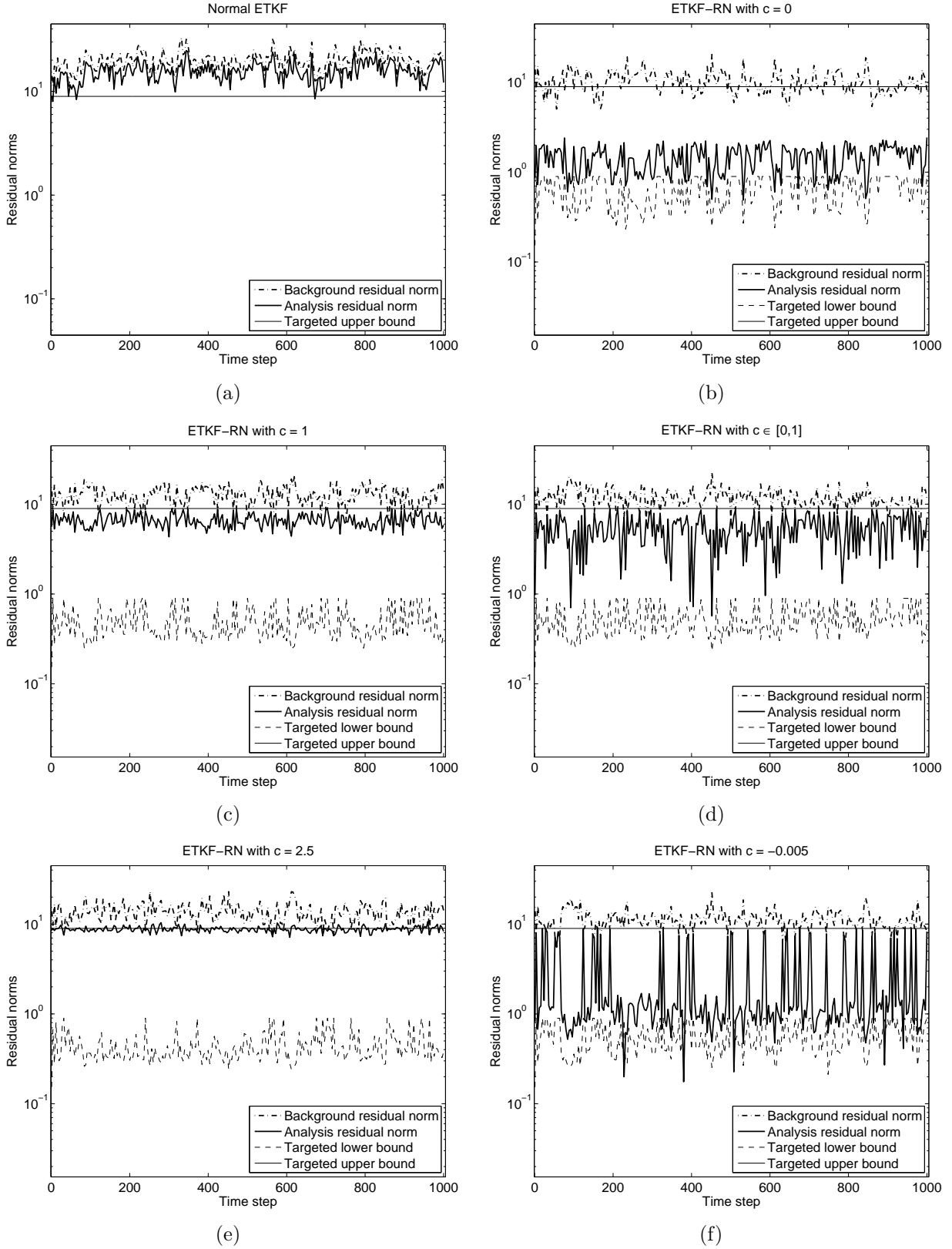


FIG. 1. Time series of the analysis residual norms in: (a): the normal ETKF without residual nudging; (b) – (f) the ETKF-RN with different c values. For the normal ETKF there are no targeted lower and upper residual norm bounds. For reference, though, we still plot the targeted upper bound ($= 2\sqrt{20}$) in (25). We also note that the c value in Fig. 1(d) is randomly drawn from the uniform distribution on the interval $[0, 1]$ at each data assimilation cycle, while in the rest of the sub-figures the c values are constant during the assimilation time window.